

Functional connectivity between motor cortex and globus pallidus in human non-REM sleep

F. Salih^{1,2}, A. Sharott³, R. Khatami⁴, T. Trottenberg¹, G. Schneider⁵, A. Kupsch¹, P. Brown⁶ and P. Grosse^{1,2}

¹Department of Neurology, Charité-Universitätsmedizin Berlin, Germany

²Interdisciplinary Sleep Disorders Centre, Charité-Universitätsmedizin Berlin, Germany

³Department of Neurophysiology and Pathophysiology, University Medical Centre, Hamburg, Germany

⁴Department of Neurology, University Hospital, Zürich, Switzerland

⁵Department of Neurosurgery, Charité-Universitätsmedizin Berlin, Germany

⁶Sobell Department of Motor Neuroscience and Movement Disorders, Institute of Neurology, London, UK

Recent evidence suggests that the motor system undergoes very specific modulation in its functional state during the different sleep stages. Here we test the hypothesis that changes in the functional organization of the motor system involve both cortical and subcortical levels and that these distributed changes are interrelated in defined frequency bands. To this end we evaluated functional connectivity between motor and non-motor cortical sites (fronto-central, parieto-occipital) and the globus pallidus (GP) in human non-REM sleep in seven patients undergoing deep brain stimulation (DBS) for dystonia using a variety of spectral measures (power, coherence, partial coherence and directed transfer function (DTF)). We found significant coherence between GP and fronto-central cortex as well as between GP and parieto-occipital cortex in circumscribed frequency bands that correlated with sleep specific oscillations in 'light sleep' (N2) and 'slow-wave sleep' (N3). These sleep specific oscillations were also reflected in significant coherence between the two cortical sites corroborating previous studies. Importantly, we found two different physiological activities represented within the broad band of significant coherence between 9.5 and 17 Hz. One component occurred in the frequency range of sleep spindles (12.5–17 Hz) and was maximal in the coherence between fronto-central and parieto-occipital cortex as well as between GP and both cortical sites during N2. This component was still present between fronto-central and parieto-occipital cortex in N3. Functional connectivity in this frequency band may be due to a common input to both GP and cortex. The second component consisted of a spectral peak over 9.5–12.5 Hz. Coherence was elevated in this band for all topographical constellations in both N2 and N3, but especially between GP and fronto-central cortex. The DTF suggested that the 9.5–12.5 Hz activity consisted of a preferential drive from GP to the fronto-central cortex in N2, whereas in N3 the DTF between GP and fronto-central cortex was symmetrical. Partial coherence supported distinctive patterns for the 9.5–12.5 and 12.5 and 17 Hz component, so that only coherence in the 9.5–12.5 Hz band was reduced when the effects of GP were removed from the coherence between the two cortical sites. The data suggest that activities in the GP and fronto-central cortex are functionally connected over 9.5–12.5 Hz, possibly as a specific signature of the motor system in human non-REM sleep. This finding is pertinent to the longstanding debate about the nature of alpha–delta sleep as a physiological or pathological feature of non-REM sleep.

(Received 2 October 2008; accepted after revision 30 December 2008; first published online 12 January 2009)

Corresponding author F. Salih: Klinik und Poliklinik für Neurologie, Charité-Universitätsmedizin Berlin, Augustenburger Platz 1, 13353 Berlin. Email: farid.salih@charite.de

Sleep is considered to be a state of cerebral activity in which the motor system is markedly inhibited, and yet physiological movements do occur. Studies of the functional organization of the motor system in human sleep are essential to better understand this seeming

paradox. In addition, a better understanding of the physiology of the motor system in sleep would also help elucidate the pathophysiological basis of sleep-associated pathological movements such as those in REM-sleep behavioural disorder (RBD), periodic limb movements

in sleep-disorder (PLMD) or sleepwalking. These can be either exclusively bound to a particular sleep stage (e.g. RBD; Schenck *et al.* 1986), or occur at regular intervals (e.g. PLMD, propriospinal myoclonus at sleep onset; Vetrugno *et al.* 2006; Montagna *et al.* 2006), or coincide with the transition from one state of vigilance to another (e.g. arousal disorders such as sleep walking). Such different clinical patterns suggest that the motor system has its own specific functional organization depending on different sleep stages. The latter assumption is further supported by investigations with transcranial magnetic stimulation (TMS), which have shown that the motor cortex can be activated by TMS in all sleep stages, but that levels of cortical excitability and inhibition differ from those in wakefulness due to sleep stage-specific modulation (Grosse *et al.* 2002; Salih *et al.* 2005).

Here we test the hypothesis that sleep stage-specific changes in the functional organization of the motor system involves both cortical and subcortical levels and that these distributed changes are interrelated within distinct frequency bands as has previously shown in rodents (Magill *et al.* 2000; Magill *et al.* 2004). In addition we assumed that these cortical–subcortical interrelations may correspond to sleep-specific coherent oscillations at the cortical level (Achermann & Borbély, 1998). To this end we evaluate connectivity between the sensorimotor cortex and a key subcortical motor structure, the globus pallidus (GP), during non-REM sleep and compare the results with the connectivity between GP and the parieto-occipital cortex as a non-motor cortical element. The GP is a component of the indirect pathway from cortex to the thalamic output nuclei being reciprocally connected to the striatum as well as to the subthalamic nucleus (STN) and substantia nigra pars reticulata (SNr). Thus the GP is in a position to substantially modify the flow of information within the basal ganglia loop (Bolam *et al.* 2000), clinically evidenced by the good response of patients with dystonia and Parkinson's disease when targeting GP with deep brain stimulation (DBS; Lozano *et al.* 2002; Kupsch *et al.* 2006).

The hypothesis that the motor cortex and the basal ganglia may be specifically coupled in sleep is based on observations from studies in animals and functional imaging. Ablation experiments in rodents destroying the striatum resulted in the alteration of normal sleep architecture (Villablanca, 1972). Further, in non-anaesthetized rats single-unit activity recordings in the STN and GP showed involvement of these two elements in the propagation of sleep specific oscillations in the low- δ -frequency range (Urbain *et al.* 2000). In sleep-like states in anaesthetized rats, Sharott *et al.* (2005) and Magill *et al.* (2004) demonstrated coherent oscillations between frontal cortex and some of the basal ganglia (STN, GP, SNr) in the range of ~ 1 Hz and sleep spindle-like elements at 7–12 Hz. Functional imaging in humans has identified specific patterns of activation and deactivation in various

cortical and subcortical regions of the brain in non-REM and REM sleep, including the principal motor nuclei of the basal ganglia (Braun *et al.* 1997; Maquet *et al.* 1997). The motor cortex is deactivated only during N3 (Braun *et al.* 1997; Maquet *et al.* 1997), whereas the basal ganglia are generally deactivated across all non-REM sleep stages. In summary, these observations contribute to the notion that the activity of the basal ganglia is specifically modulated in sleep.

In the present study, we investigate changes in the functional connectivity between cerebral cortex and GP during non-REM sleep in drug-free patients without sleep-related complaints undergoing DBS for generalized or segmental dystonia. Our assumption was that the oscillatory drives we would identify reflect a physiological state and not that of the dystonic pathology. This assumption is based on the fact that dystonic symptoms usually subside in sleep (Brotini & Gigli, 2004), but also, as detailed below, our inability to identify pathological 3–10 Hz coherent oscillations involving GP, which have been shown in patients with dystonia (Sharott *et al.* 2008) while patients were sleeping. However, as in previous investigations studying DBS patients, we cannot entirely rule out minor confounding effects of local GP trauma due to the DBS electrode implantation or long-term pharmacological effects on synaptic activity which might potentially influence functional coupling even after drugs are washed out completely. So far, sleep recordings in patients undergoing DBS have proven informative about the nature of thalamic involvement in the generation and maintenance of sleep or the propagation of epileptic activity (Tsoukatos *et al.* 1997; Velasco *et al.* 2002; Wennberg & Lozano, 2003), but have not been used to investigate functional connectivity in sleep within a functional system such as the motor system.

Methods

Patients and methods

Ethical approval. The study was approved by the Charité-Medical University Berlin Ethics Committee and conforms to the standards set by the *Declaration of Helsinki*. All subjects (and parents of case 4) gave written informed consent.

Patients and healthy subjects. We examined both hemispheres in seven patients ($n = 14$; six men, one woman; mean age: 42.3 ± 16.9 , range: 17–74 years) in whom DBS electrodes were inserted in GP to treat generalized or segmental dystonia. Clinical details are given in Table 1. Cases 1 and 2 were siblings and cases 3 and 4 were DYT-1 positive. Patients did not receive any drugs interfering with sleep after surgery and did not complain of

Table 1. Patient's clinical details

Case	Sex	Age (years)	Disease duration (years)	Distribution	Aetiology	DYT-1	Pre-op BFM-score ¹	Pre-op imaging (MRI)	Medication prior to surgery
1	M	41	22	Segmental	Hereditary	no	12	Normal	None
2 ^{3,4,5}	M	36	29	Generalized	Hereditary	no	82	Slight generalized atrophy	Haloperidol Tiaprid Lorazepam
3 ^{3,4}	M	42	15	Generalized	Hereditary	yes	69	Normal	None
4	M	17	10	Generalized	Idiopathic	yes	75	Normal	None
5	F	46	30	Segmental	Idiopathic	na ²	15	Normal	Tetrazepam
6	M	40	1	Segmental	Idiopathic	na	10	Normal	Metoprolol Primidone
7 ^{3,4}	M	74	13	Segmental	Idiopathic	na	12	Normal	Tilidin

¹Burke–Fahn–Marsden rating scale-score motor; ²not assessed; ³previously also reported in Sharott *et al.* (2008); ⁴previously also reported in Chen *et al.* 2006a; ⁵previously also reported in Chen *et al.* 2006b.

any prior sleep disorder or sleep problem during the night of the recording. The surface EEG findings in the patients were compared to those in seven age- and sex-matched healthy subjects (mean age: 40.1 ± 15.9 years; range: 16–69 years).

Patients were recorded in the interval between DBS implantation and subsequent connection to a subcutaneously placed stimulating device. The operative procedures have been described elsewhere (Vitek *et al.* 1999; Volkmann & Benecke, 2002; Krauss *et al.* 2003). DBS electrodes were inserted bilaterally. The DBS electrode used was model 3387 (Medtronic Neurological Division, Minneapolis, MN, USA) with four platinum–iridium cylindrical surfaces (1.27 mm diameter and 1.5 mm length) and centre to centre separations of 3 mm. Contact 0 was the lowermost and contact 3 the uppermost contact. Pallidal electrode trajectories were aimed at the postero-ventral portion of the GP and the posterior ansa lenticularis. The target was identified on high resolution T2-weighted axial, coronal and sagittal MRI planes. These images were superimposed on coronal and lateral contrast ventriculography and drawn on the GP Tailairach Scheme, corresponding in location to the GP area in the Schaltenbrand and Wahren atlas (Schaltenbrand & Wahren, 1977). The depth of the lowest contact was aimed to be at least 1 mm above the upper border of the optic tract. The location of the latter was established using intraoperative induction of visual phosphenes by high frequency stimulation and/or the measurement of electrical activity from the optic tract. Intra-operative microelectrode recordings and macrostimulation were performed in all patients. The target coordinates for the lower contact were 2–3 mm in front of the mid-commissural point, 20–22 mm lateral to the midline of the third ventricle and 4–6 mm below the anterior commissure (AC)–posterior commissure (PC) line.

Recordings

All-night polysomnography was performed 5–9 days after stereotaxic implantation of DBS electrodes. Local field potentials (LFP) were recorded from GP of both hemispheres using a bipolar montage of the contacts of each DBS electrode. Surface EEG was recorded bipolarly from fronto-central (F3–C3; F4–C4; in the following: fc) and parieto-occipital (Pz–O1; Pz–O2; in the following: po) cortical areas, according to the 10–20-system. Submental EMG and EOG were additionally recorded to appropriately assess sleep stages. The sampling rate was 1000 Hz. LFPs and EEG were pass-band filtered at 1 and 250 Hz and amplified ($\times 100\,000$). Signals were amplified and filtered using a custom-made 9 V battery-operated portable high-impedance amplifier (which had as its front-end input stage the INA128 instrumentation amplifier; Texas Instruments, Dallas, TX, USA) and recorded through a 1401-A/D converter (Cambridge Electronic Design, Cambridge, UK) onto a portable computer using Spike2, version 5. Sleep stages were designated according to the criteria proposed by the American Academy for Sleep Medicine (2007). The latter modified some of the rules established by Rechtschaffen & Kales (1968), e.g. N3 instead of S3 or non-REM 3, fusing the former S3 and S4, equal to the term slow-wave sleep, to one single stage termed N3. Sleep data were drawn from the first two sleep cycles. EEG in wakefulness was recorded in the same session prior to starting polysomnography with the patients lying in bed with their eyes closed.

Analysis

FFT-based frequency analysis was based on continuous arousal-free 200 s of recording for each state of vigilance (wakefulness, N2, N3, REM) in the frequency range from 0.5 to 40 Hz with a frequency resolution of ~ 0.25 Hz as

in Achermann & Borbély (1998). As in REM sleep no significant coherence was present for any topographical constellation (data not shown), no further analysis was performed for that sleep stage. MAR-based frequency analysis was based on the first 80 s of continuous recording used for FFT-based analysis and had a frequency resolution of 0.4 Hz. As in previous studies (Achermann & Borbély, 1998), power and coherence spectra below 0.5 Hz were excluded from the analysis because of the overlap between physiological cerebral activity and artefacts from eye movements and respiration. For analysis we selected the LFP contact pair in each GP which exhibited the highest power in the frequency range for sleep spindles in N2. Sleep spindles define the initiation of stable sleep and are not prone to obscuration by artefacts as might be the case for other sleep specific elements such as K-complexes or high amplitude δ -waves.

Power and coherence

Power and coherence were analysed off-line using a program written by J. Ogden and D. Halliday (Division of Neuroscience and Biomathematical Systems, University of Glasgow, UK) based on methods outlined by Halliday *et al.* (1995). The EEG, denoted by subscript a, and rectified EMG, denoted by subscript b, were assumed to be realizations of stationary zero mean time series. The statistical tool used for data analysis was the discrete fast Fourier transform (FFT) and parameters derived from it. These were estimated by dividing the records into a number of disjoint sections of equal duration (4096 data points) and estimating spectra by averaging across these discrete sections. In the frequency domain estimates of the autospectrum of the EEG, $f_{aa}(\lambda)$, and EMG, $f_{bb}(\lambda)$ and their cross-spectrum, $f_{ab}(\lambda)$ were constructed. The coherence, $|R_{ab}(\lambda)|^2$, was also estimated:

$$|R_{ab}(\lambda)|^2 = \frac{|f_{ab}(\lambda)|^2}{f_{aa}(\lambda)f_{bb}(\lambda)}$$

where coherence is a measure of the linear association between two signals. It is a bounded measure taking values from 0 to 1 where 0 indicates that there is no linear association (that is process B is of no use in linearly predicting process A) and 1 indicates a perfect linear association. The variance of the coherence was normalized by transforming the square root of the coherence (a complex valued function termed coherency) at each frequency using the Fisher transform. This results in values of constant variance for each record given by $1/2L$ where L is the number of segment lengths used to calculate the coherence. Data were then pooled for each group and the 95% confidence limits of the mean calculated.

DTF

The directed transfer function (DTF) investigates any possible asymmetry in the flow of coherent activity between signals (Kaminski & Blinowska, 1991; Mima *et al.* 2001). To this end, the multiple autoregressive (MAR) model that best described the signals coming from the two regions of interest was determined. The MAR methodology is essential for the DTF, as the DTF is built directly from the MAR coefficients. Following the procedure detailed in Cassidy & Brown (2003), a Bayesian methodology was applied to estimate the parameters of the autoregressive model. This approach is desirable in that it provides full probabilistic distributions for all of the model parameters. In addition, the complexity of the model (i.e. the most appropriate number of spectral peaks) is determined objectively and automatically based on the data supplied to the model (for further details see Cassidy & Brown, 2003; Sharott *et al.* 2008). The autoregressive coefficients can be used to construct a bounded, normalized measure (the DTF) that provides information on the effective direction of coupling. The off-diagonal MAR coefficients indicate the temporal coupling between one site and another, and (depending on whether they are upper or lower off-diagonal) the direction of that coupling. By squaring and normalizing the MAR coefficients the DTF is obtained, as described by Kaminski & Blinowska (1991).

Where the DTF of coherent activity at two recording sites is symmetric, no effective direction of coupling predominates, either because phase delays of mixed coherent activities are balanced, or volume conduction occurs or there is genuine biological synchronization with zero phase (and time) difference (Cassidy & Brown, 2003). Where the DTF of coherent activity at two recording sites is asymmetric, the 'effective direction of coupling' predominates in one direction and coherent activity or activities in one population of neurons tend to lead in time. It should be noted, however, that an asymmetrical DTF does not necessarily imply a direct connection between the two areas in which activity is recorded. Thus, information can be transferred indirectly between recorded structures, via one or more unrecorded structures, or indeed, activity in both recorded structures may be driven by a third unrecorded structure. The relative time delays between different structures and intermediate relays may also influence the effective direction of coherent activity. As such, the interpretation of the DTF has to be functional connectivity (Sharott *et al.* 2005 and see Discussion).

Here we used bivariate, as opposed to multivariate, DTF analysis where all available channels are used to produce one MAR model. Some methodological and experimental studies advocate the use of multivariate analysis (Korzeniewska *et al.* 2003; Supp *et al.* 2005) and even suggest bivariate analysis may lead to spurious results

(Kus *et al.* 2004). However, the potential advantages of the multivariate model can only be fully realized if all, or at least many, strategically important nodes in a circuit can be recorded. This is difficult to achieve when studying the cortico-basal ganglia network in human subjects, even those with deep brain electrodes. In addition, the interpretation of the bivariate DTF is fairly straightforward (Sharott *et al.* 2005) and was more complementary to the other pairwise spectral analyses used here.

In addition, a general concern in all DTF analyses is whether spurious asymmetries of information flow can be generated through a poor signal to noise ratio (SNR) in one or more of the signals under consideration. This issue has been evaluated with respect to EEG where it has been noted that estimates are reasonable provided SNRs ≥ 3 and ≥ 4800 data samples are available (Astolfi *et al.* 2005). Our data sets far exceeded this sample limit and the SNR of LFP signals likely exceeds that of EEG (Regan, 1989).

Partial coherence

First-order partial coherence functions were estimated to assess whether 'partialization' with a third process (the 'predictor') accounted for the relationship between two other processes (Halliday *et al.* 1995; Rosenberg *et al.* 1998). As used here, partial coherence represents the fraction of coherence between one signal (e.g. left GP) that is not shared by the other two (e.g. F3–C3 and Pz–O1). Thus, if sharing of the one signal (left GP) between the other two signals (F3–C3 and Pz–O1) were complete, then partialization of GP as the predictor with surface EEG would lead to zero coherence. It follows that if GP had no influence on the coupling of surface EEG then partialization would have no effect on the coherence of the surface EEG. Two issues should, however, be highlighted. First, the partial coherence function is based on the assumption of linearity, so that failure in the partial coherence to drop compared to the ordinary coherence does not exclude non-linear interactions between the different signals. Second, partialization occasionally leads to an increase in coherence between two signals. This occurs when the predictor has little temporal coupling with the two signals of interest, so that removal of its effect by partialization is equivalent to eliminating a 'noise term' from the coherence between the two signals of interest (Lopes da Silva *et al.* 1980).

Statistical analysis

To compare transformed FFT-based coherences between groups a repeated measures General Linear Model was performed using frequency bands and sites (fc–po, GP–fc, GP–po) as the main effect. To this end transformed coherences were averaged across 0.5–4 Hz,

4–9.5 Hz, 9.5–12.5 and 12.5–17 Hz. These bands were selected because they represent sleep specific frequency ranges, i.e. 1 and 2–4 Hz- δ -waves, θ - and low α -activity, high- α -activity, and sleep spindles, respectively. Where results were non-spherical, a Greenhouse–Geisser correction was used and when differences were significant at the group level *post hoc* pair-wise comparison with Scheffé's correction was carried out.

Results

EEG

Figure 1 is a representative example of the signals recorded from case 1 in all three states of vigilance. Wakefulness with eyes closed was dominated by an almost regular parieto-occipital rhythm at ~ 10 Hz while in the fronto-central lead higher frequencies at ~ 20 Hz prevailed with interspersed waves in the α -frequency band, and to a minor extent also in the θ -frequency band. LFPs from GP were of much lower amplitude than the surface EEG, but showed quite similar frequency patterns to fronto-central leads.

In N2 sleep a mixture of K-complexes, sleep spindles in the frequency range of 13–17 Hz and 2–4 Hz low amplitude δ -waves could be identified in fronto-central and parieto-occipital leads. K-complexes could coincide in both EEG leads, but did not necessarily do so at all times. In the LFP from GP, δ -waves of about 0.8 s duration coincided with and matched the duration of K-complexes in the surface EEG. In addition, grouped waves in the β -frequency band ~ 15 Hz were present.

In N3 sleep surface EEG showed high amplitude δ -waves of 0.8–0.9 s duration along with some 2–4 Hz δ -waves. Both elements appeared with higher density and with higher amplitudes compared to N2 and high amplitude δ -waves reached up to 40% of any epoch. Additionally, spindle-like activity appeared in both leads, usually time locked to high-amplitude δ -waves. Another grouped activity at ~ 10 Hz was only present in fronto-central leads. In the LFP from GP δ -activity was occasionally present, though not synchronous with the surface EEG. However, the LFP was dominated by ~ 15 Hz and ~ 10 Hz activity which appeared to be synchronous with that in the fronto-central leads.

Power spectra (Fig. 2)

Pooled power spectra from all subjects confirmed the above patterns. In parieto-occipital cortex (Fig. 2A) a large 8–10 Hz peak appeared in wakefulness. This was double-shaped because of interindividual variation in the frequency of the peak in this range. In eight hemispheres (four patients) the peak frequency was between 7.5 and 8.5 Hz while in six hemispheres (three patients) it was

from 9.7 to 10.2 Hz. In parieto-occipital cortex during N2 there was a peak in the frequency range of sleep spindles at 14.2 Hz. A similar peak in N3 was of slightly lower frequency at 13.7 Hz and was preceded by a peak between 10 and 12 Hz. The latter was not evident in N2.

In the fronto-central cortex (Fig. 2*B*), during wakefulness the pattern was similar to that in parieto-occipital cortex, although the double peak at

8–10 Hz was of smaller amplitude. In N2 two peaks at 10–12 and 14.5 Hz were present, while in N3 the 10–12 Hz peak persisted and the ~14 Hz peak diminished. Power spectra of the GP (Fig. 2*C*) substantially differed from those of surface EEG. In wakefulness the power spectrum had no distinct peak except in the δ - and low θ -range. In N2 and N3 a peak between 10 and 12 Hz appeared. As for the fronto-central cortex, this peak shifted slightly to lower

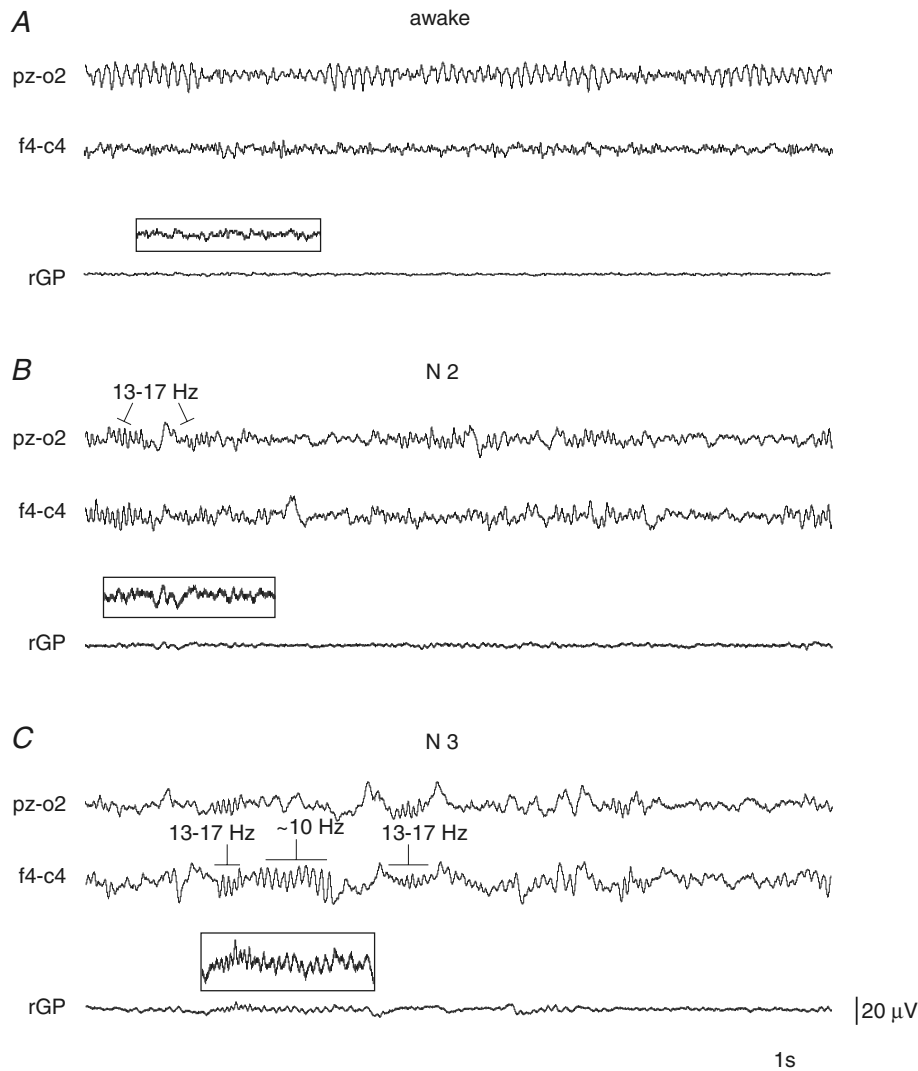


Figure 1. Right-sided surface EEG and LFP from right GP of case 1 in the three states of vigilance (awake, N2 and N3)

A, wakefulness: a regular α -rhythm of ~9 Hz is present in Pz–O2, while in F4–C4 frequencies in the β -frequency band dominate with interspersed waves in the α - and to a minor extent θ -band. LFPs from GP compared to surface EEG (see box for LFP amplified a further 3 times) are of very low amplitude and show similar frequencies as seen in fronto-central leads. *B*, N2: both surface EEG traces consist of K-complexes, sleep spindles between 13 and 17 Hz and waves in the θ -frequency range. Activities in Pz–O2 and F4–C4 are partially synchronized. K-complexes can also be identified in the GP-LFP. Boxed area as in *A*. *C*, N3: low frequency δ -waves (~1 Hz) are of higher amplitudes than in N2 (note that δ -waves here are smaller than the 75 μ V required for N3 according to Rechtschaffen & Kales (1968), because a bipolar lead is used in contrast to the usual contralaterally placed ear reference). Both surface EEG traces appear to be more synchronized than in N2. In addition to sleep spindles in the range of 13–17 Hz, ~10 Hz spindle-like waves are also present in F4–C4, but not in the parieto-occipital lead. In GP both sleep spindles as well as the ~10 Hz activity are present, mostly in synchrony with F4–C4. Boxed area as in *A*.

frequencies in N3 (10.7 Hz) compared to N2 (11.7 Hz). Finally, all leads showed a peak between 0.75 and 1.5 Hz for both non-REM sleep stages, being highest in N3 for all three sites.

Coherence (Fig. 3)

Coherence spectra between fronto-central and parieto-occipital cortex, GP and fronto-central cortex and GP and parieto-occipital cortex were dominated by a broad-based peak centred in the α -frequency range (7–12 Hz) during wakefulness (Fig. 3A). This was more prominent in the surface EEG than between GP and cortical sites.

In N2 (Fig. 3B) the coherence between fronto-central and parieto-occipital cortex had a major peak between 12.5 and 17 Hz with a maximal value at 14.7 Hz. This was preceded by a small peak at 10–12 Hz. The latter was enhanced in the coherence between GP and fronto-central cortex, while the 13–17 Hz peak was relatively suppressed. Both peaks were present in the coherence between GP and parieto-occipital cortex. The coherence between the fronto-central and parieto-occipital cortex also demonstrated a small peak between 2 and 4 Hz.

In N3 sleep (Fig. 3C) the pattern of coherence between EEG sites was very similar to that in N2, with a major 13–17 Hz peak preceded by a minor 10–12 Hz peak. In contrast, the peak at 13–17 Hz almost disappeared in the coherence between GP and fronto-central cortex and GP and parieto-occipital cortex. The \sim 10–12 Hz peak persisted in all spectra. Different from N2, there was a small δ -coherence peak in all constellations but at a low peak-frequency ($<$ 2 Hz). The pattern of coherence in N2 and N3 was further evaluated by comparison of the mean transformed coherence over the δ -frequency band and over the frequency ranges of 4 and 9.5 Hz, 9.5–12.5 Hz and 12.5–17 Hz. Separate general linear models for N2 and N3 showed significant interactions between frequency bands and sites (N2: $F_{2,15,27,90} = 12.70$; $P < 0.0005$ and N3: $F_{2,07,26,87} = 8.48$; $P < 0.0005$). The *post hoc* comparisons between frequency bands in the different pairs of sites are summarized in Fig. 3D and E and confirmed multiple differences. In essence, between fronto-central and parieto-occipital cortex, coherence in the sleep spindle range differed from that in all other ranges in both N2 and N3. Between GP and both cortical sites the coherence in the high α -range differed from that in adjacent frequency ranges in both N2 and N3. There was no difference in coherence between cortical sites between patients and healthy subjects for any frequency range (data not shown).

In line with a previous study (Achermann & Borbély, 1998) no significant coherence was present for any topographical constellation in REM sleep.

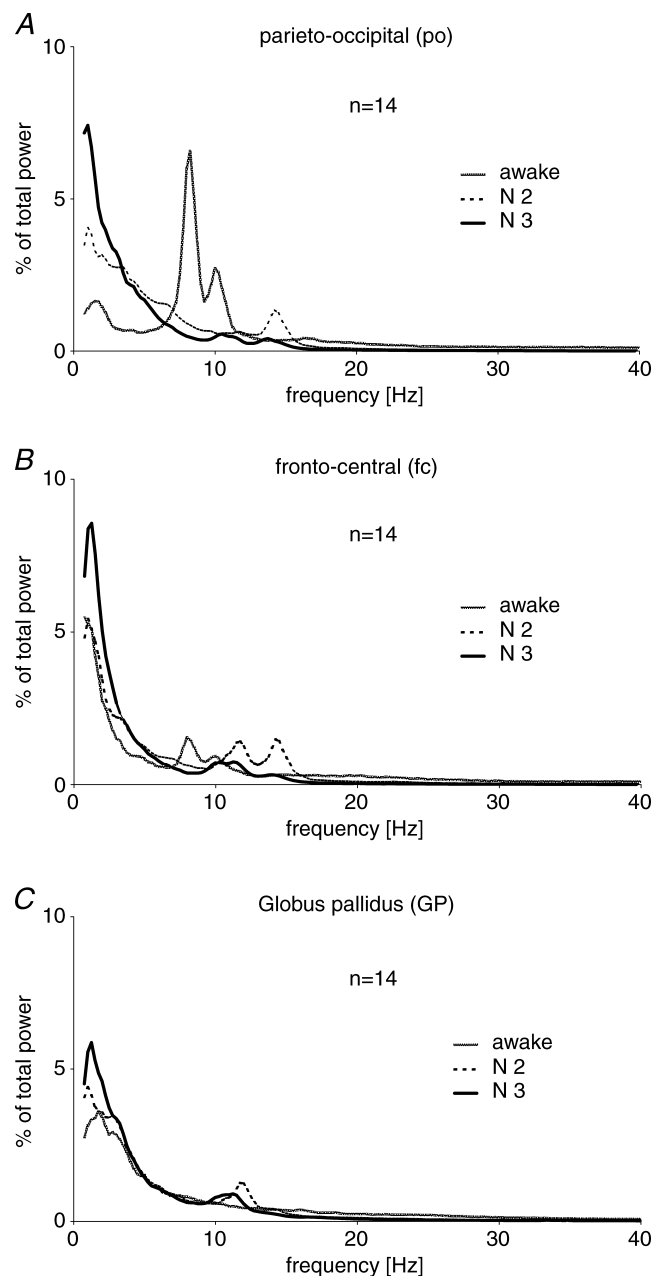
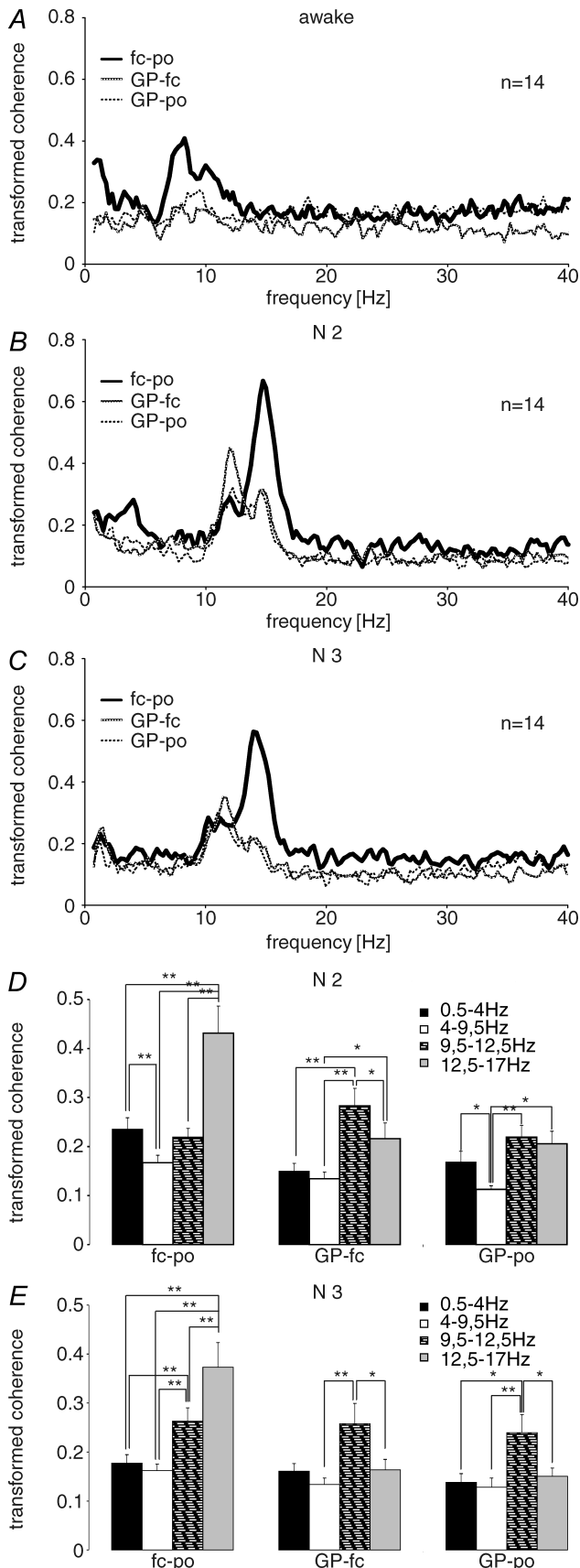


Figure 2. Group averaged power spectra of the three recording sites in the three states of vigilance

Power spectrum for the parieto-occipital (po) cortex (A) in wakefulness is dominated by a very high 7–12 Hz double-shaped peak. In N2 a clear \sim 14 Hz peak is present while in N3 a 10–12 Hz peak precedes a minor 12–14 Hz peak. In both non-REM sleep stages, power peaks between 0.75 and 1.5 Hz, more prominent in N3. In the fronto-central (fc) cortex (B) a broad-based 7–12 Hz double peak is present in wakefulness as in the parieto-occipital lead. In N2 dominant peaks occur between 0.75 and 1.5 Hz and between 10 and 12.5 Hz as well as between 12.5 and 15 Hz. In N3 only the distinct peaks between 9.5 and 12 Hz and 0.75 and 1.5 Hz remain, with the latter being again higher than in N2. The spectrum in GP (C) differs from surface EEG as in wakefulness there is no clear peak, while in N2 and N3 the only peaks are at \sim 10–12 Hz and between 0.75 and 1.5 Hz. Similar to both cortical sites, power between 0.75 and 1.5 Hz was most pronounced in N3.



Directed transfer function (Fig. 4)

The DTF was used to identify asymmetric drives between sites at frequencies which revealed functional coherence. More specifically we aimed at using DTFs to help address whether the spectral feature at ~ 10 – 12 Hz was a variation of sleep spindles with just a lower frequency than classical spindles, or had a different physiological basis. DTFs revealed a characteristic pattern. In both N2 and N3, drives from GP had a peak frequency in the 10–12 Hz frequency range whereas drives from parieto-occipital cortex tended to peak over the higher frequency band (12.5–17 Hz). The drive from GP at 10–12 Hz was most prominent between GP and fronto-central cortex in N2, when it also exceeded the drive in the opposite direction. In contrast, the drive from parieto-occipital cortex at or above 12.8 Hz always exceeded that in the opposite direction in both N2 and N3. DTF in the δ -range showed an asymmetric drive with a peak at < 2 Hz from fronto-central cortex to GP in N2 which was enhanced in N3. Data from wakefulness are not shown, but DTF spectra demonstrated peaks at 8.4 Hz in both directions between both cortical sites, and from parieto-occipital cortex to GP, but not between fronto-central cortex and GP or from GP to parieto-occipital cortex.

Partial coherence (Figs 5 and 6)

Partial coherence was used to complement the DTF in the differentiation of the 10–12 Hz activity from higher

Figure 3. Group averaged transformed coherence spectra between recording sites in the three states of vigilance

In wakefulness (A) the coherence spectrum for surface EEG (fc-po) shows a broad-based double-shaped peak between 7 and 12 Hz. For the combinations between GP and the two cortical sites the same peaks are present, though they are much smaller. In N2 (B), coherence between both cortical sites shows a prominent 13–17 Hz peak, preceded by a peak at 10–12 Hz. Coherence between both cortical sites also peaks at 2–4 Hz, but at a lower level. Between GP and the fronto-central cortex the 10–12 Hz peak exceeds that seen between both cortical sites and is also more pronounced than the 13–17 Hz peak. Both coherence peaks are also present between GP and parieto-occipital cortex, but are more similar in height. No coherence peak is seen in the δ -range in coherences involving the GP in N2. In N3 (C), the same 13–17 Hz peak is present in the coherence between both cortical sites; however, the peak frequency is slightly lower than in N2. The 10–12 Hz peak remains present. In coherences between GP and the two cortical areas, the 13–17 Hz peak is almost indiscernible while the 10–12 Hz peak persists. In all three constellations, there was a small peak in the delta range but at a low peak frequency (< 2 Hz). Statistical analyses for N2 (D) and N3 (E) show multiple significant differences. Of particular importance is the fact that between fronto-central and parieto-occipital cortex the sleep spindle range (12.5–17 Hz) coherence was bigger than that in other ranges, while between GP and fronto-central cortex 9.5–12.5 Hz coherence was bigger than that in adjacent frequency ranges during N2 and N3. The coherence between GP and parieto-occipital cortex followed a similar pattern.

frequency spindle-related activity. Figure 5 exemplifies the findings in the patient previously illustrated in Fig. 1. For the peak between 9.5 and 12.5 Hz in N2 and N3 coherence between both cortical sites dropped to $\sim 30\%$ of its original value after partialization with GP as the predictor (Fig. 5A). For the same peak, coherence between GP and fronto-central cortex dropped to 86% in N2 and to 57% in N3 when the parieto-occipital cortex was used as the predictor (Fig. 5B). Similarly, the coherence between GP and parieto-occipital cortex dropped to $\sim 63\%$ when fronto-central cortex was used as the predictor (Fig. 5C). On the other hand, the effect of partialization with GP as predictor on coherence between both cortical sites was negligible in the frequency range of sleep spindles (12.5–17 Hz), either in N2 or N3 (Fig. 5A). However, using either of the two cortical sites as predictor, coherence between GP and the remaining cortical site was almost halved during N2 in the 12.5–17 Hz frequency band.

These patterns could not be seen in every patient and in every hemisphere (Fig. 6). Despite this, however, the general pattern described above was born out by analysis. When partializing out the effect of GP activity on the coupling between fronto-central and parieto-occipital, coherence in the 9.5–12.5 Hz range dropped by $> 10\%$ in 9 out of 14 hemispheres in N2, in 8 out of 14 hemispheres in N3 and in 11 out of 14 hemispheres in either N2 or N3. In contrast, there was no such drop in coherence with GP as predictor over the frequency range of sleep spindles in any of the patients, either in N2 or N3. These differences in the effects of partialization between the two frequency ranges were significant (Fisher's exact test; N2, $P < 0.001$; N3, $P = 0.001$; N2 or N3, $P < 0.001$).

Discussion

We have shown significant coherence between GP and fronto-central cortex and GP and parieto-occipital cortex in circumscribed frequency bands from 9.5 to 17 Hz in N2 and N3 as well as in the δ -frequency band in N3. This pattern differs from that in wakefulness so that the coherence pattern should be considered sleep specific. Importantly, there appear to be two different physiological activities represented within the broad band of significant coherence from 9.5 to 17 Hz in non-REM sleep. As expected, there is a component in the frequency range of sleep spindles (12.5–17 Hz) with a maximum centred at ~ 14 Hz. This was best seen in the coherence between both cortical sites and that between GP and cortical sites during N2, and in surface-EEG coherence during N3. The DTF suggested that the spindle frequency component was preferentially driven from parieto-occipital cortex. The second component consists of an activity in the 9.5–12.5 Hz band. Coherence was elevated in this band for all topographical constellations in both N2 and N3, but

especially between GP and fronto-central cortex. The DTF further suggested that the 9.5–12.5 Hz activity consisted of a preferential drive from GP to the fronto-central cortex in N2 and a more symmetric drive between sites in N3. Partial coherence supported the impression of distinctive patterns of drive for the 9.5–12.5 Hz and 12.5–17.0 Hz components, so that coherence in the 9.5–12.5 Hz band was reduced when the effects of GP were removed, whereas coherence in the 12.5–17.0 Hz band dropped when the effects of both cortical sites were removed. In essence, our evidence suggests that GP and frontal cortex are functionally coupled at ~ 10 –12 Hz, possibly as a specific signature of the motor system in non-REM sleep. The latter is pertinent to the longstanding debate on 'slow' and 'fast' sleep spindles as well as to the problem of alpha-delta sleep as a physiological or pathological feature of non-REM sleep. As our study was limited to frequencies below 40 Hz some coherence patterns above this frequency were potentially not detected. This may be the reason why REM-sleep did not show any coherent activities in the current investigation.

Coherence in the frequency range of sleep spindles

Our study confirms the presence of synchrony in non-REM sleep between the fronto-central and the parieto-occipital cortex in the frequency range of sleep spindles centred around 14 Hz (Achermann & Borbély, 1998; Duckrow & Zaveri, 2005). Also, in keeping with previous studies, we found the peak frequency in N2 to be higher by ~ 1 Hz compared to N3 (Olbrich & Achermann, 2005) as well as the overall level of coherence in N2 to be higher than in N3. As reported before, the ~ 14 Hz peak in the coherence spectrum was also reflected in the respective power spectra (Achermann & Borbély, 1998; Duckrow & Zaveri, 2005). The DTF suggested that the main drive in the 13–17 Hz range was directed from the parieto-occipital cortex to the frontal cortex. However, the results of signals analysis techniques such as the DTF and partial coherence must be considered in the context of other lines of evidence. Sleep spindles are generated in the reticular thalamic nucleus (RTN) and then trans-synaptically driven from there through other thalamic sites to cortex (Guillery & Harting, 2003). With the RTN as the common generator of sleep spindles, coherence between two cortical sites may well be present at ~ 14 Hz as an indication of a common input to both sites through thalamo-cortical connectivity (Contreras *et al.* 1996; Achermann & Borbély, 1998). In this case, the apparent DTF drive from parieto-occipital cortex to frontal cortex may result from a shorter effective conduction delay from thalamus to parieto-occipital cortex.

Interestingly, we also found a coherence peak in the frequency range of sleep spindles to be present between

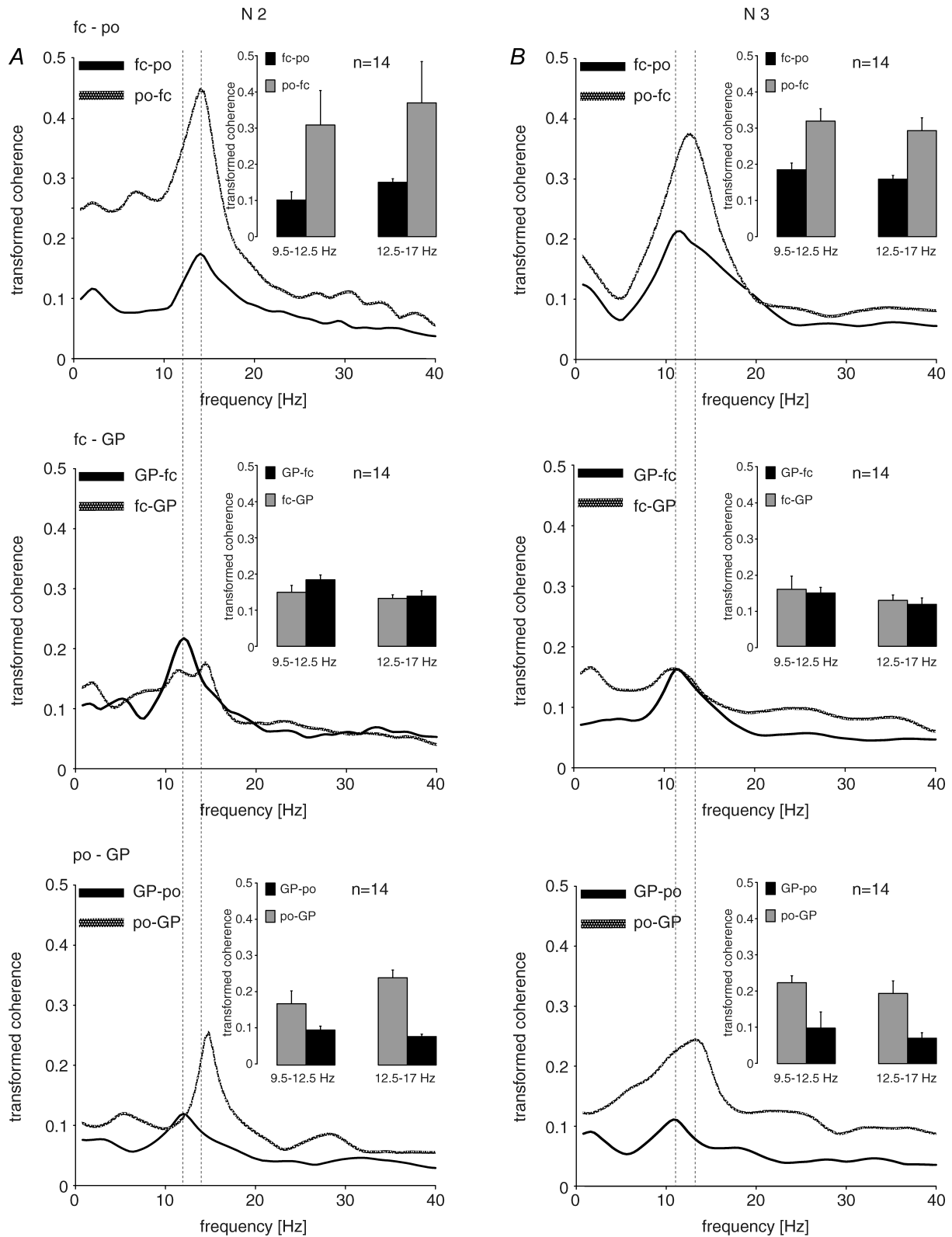


Figure 4. Pooled results for DTF (directed transfer function) for N2 and N3 for the various combinations of the three recorded sites

Lines indicate directed (transformed) coherence spectra, insets averaged coherences for the frequency bands of 9.5–12.5 and 12.5–17.0 Hz, respectively. Each figure represents the directed coherence from one site to another

GP and both cortical sites in N2, though at a lower level compared to between surface EEG sites. In N3 this peak almost disappeared, though a very large peak persisted in surface EEG. This constellation raises the possibility that GP is integrated into the network through which sleep spindles are propagated in N2, and to a lesser extent in N3. The fact that the power spectra of GP did not show a distinct peak in the range of sleep spindles does not necessarily argue against this possibility as there is no strict correlation between power and coherence. The DTFs between GP and either of the cortical sites were asymmetric in the frequency range of sleep spindles, with flow from cortex dominating. Similarly, coherence between cortical sites was relatively unaffected by the use of GP as predictor. Given the evidence discussed above these findings are best resolved by a thalamic spindle generator that has a fast and strong projection to cortex (perhaps fastest to parieto-occipital cortex) and a slow and weaker projection to GP. These findings might suggest that sleep-spindle oscillations also contribute to initiate sleep-specific activity changes within basal ganglia networks. Furthermore, once stable sleep activity is projected through basal ganglia networks these oscillations are then replaced by synchronized δ -oscillations as well as by the activity in the 10–12 Hz range. During slow-wave sleep (N3) the latter might fulfil a more specific functional role for motor system organization than sleep-spindle oscillations (see below).

Coherence in the δ -frequency range

Functional connectivity in the δ -range occurred at a much lower level compared to coherences related to sleep spindles and the 10–12 Hz activity. All leads recorded in our study showed a power peak in the low δ -range (between 0.5 and 1.5 Hz) for both non-REM sleep stages, which was highest in N3. Coherence patterns differed between in N2 and N3. Thus, different δ -oscillations as characterized in sleeping cats (Steriade, 2000; Steriade, 2001) might also be present in humans. In N2 significant coherence was only present between the two cortical sites between 2 and 4 Hz, but not between GP and cortex. Conversely, in N3 a small δ -coherence peak could also be seen in topographical constellations involving GP. However, this coherence peaked at a lower peak frequency (< 2 Hz) than in N2. DTFs showed asymmetric drives with predominant coherence from cortex to GP in N3,

especially from fronto-central cortex to GP. This pattern is consistent with previous evidence suggesting that slow oscillations in the δ -frequency range are predominantly projected through frontal lobe networks (Werth *et al.* 1997; Finelli *et al.* 2001; Steriade, 2001). Our data suggest that basal ganglia like the GP might also be involved in sleep-specific δ -coupling.

Functional coupling in the 10–12 Hz band

While coherence patterns in the spindle range between GP and cortex are likely to be explained by a common 'third' generator, our results for the peak in coherence at ~10–12 Hz are consistent with more direct functional coupling between GP and the motor cortex in non-REM sleep. It has long been established that ~10 Hz activity can be a feature of non-REM sleep in surface EEG (for review see Pivik & Harman, 1995), particularly during N3. However, the significance of these ~10 Hz oscillations had been unclear until recently. They were originally regarded as a pathological element in the EEG of patients with psychiatric or musculoskeletal disorders, termed 'alpha-delta sleep' or 'alpha EEG non-REM sleep anomaly' (Hauri & Hawkins, 1973; Moldofsky, 1989). Subsequently, this 'alpha-intrusion' was equated with a hyperarousable state as any activity in the α -frequency band was assumed to be necessarily related to wakefulness, or a tendency towards it, driven by the occipital cortex. Yet other studies pointed out that ~10 Hz activity can occur in healthy subjects free of any sleep-related complaints (Scheuler *et al.* 1983). Recent investigations using signal analysis have re-examined the role of ~10–12 Hz oscillations in non-REM sleep and conclude that they are a physiological sleep feature of non-REM sleep (Pivik & Harman, 1995) with a preferential spatial distribution in the frontal and central leads (Duckrow & Zaveri, 2005). We also found this alpha activity to be coherent between fronto-central and parieto-occipital cortex in N3, and to a lesser extent in N2, which is in line with previous results (Achermann & Borbély, 1998).

Other relevant studies have investigated the role of fast *versus* slow sleep spindles, the former with a peak between 11 and 12 Hz, the latter at around 14 Hz, described for the first time by Gibbs & Gibbs (1950). Though frequency ranges indicated by different authors may vary between 9 and 13 Hz for the slow spindles and terminology has been inconsistent (see, e.g. Dijk *et al.* 1995; Scheuler,

and that in the opposite direction. Peak frequencies from GP to other sites are always in the range of 9.5–12.5 Hz. Flows from parieto-occipital cortex always peak in the higher frequency band for sleep spindles (13–17 Hz). The peak at 9.5–12.5 Hz linked to GP becomes most prominent when the DTF from GP to fronto-central cortex is considered in N2. DTF in the δ -range showed an asymmetric drive peaked at < 2 Hz from fronto-central cortex to GP in N2, which was even more enhanced in N3. Coherences are much higher in drives from parieto-occipital cortex to all other sites.

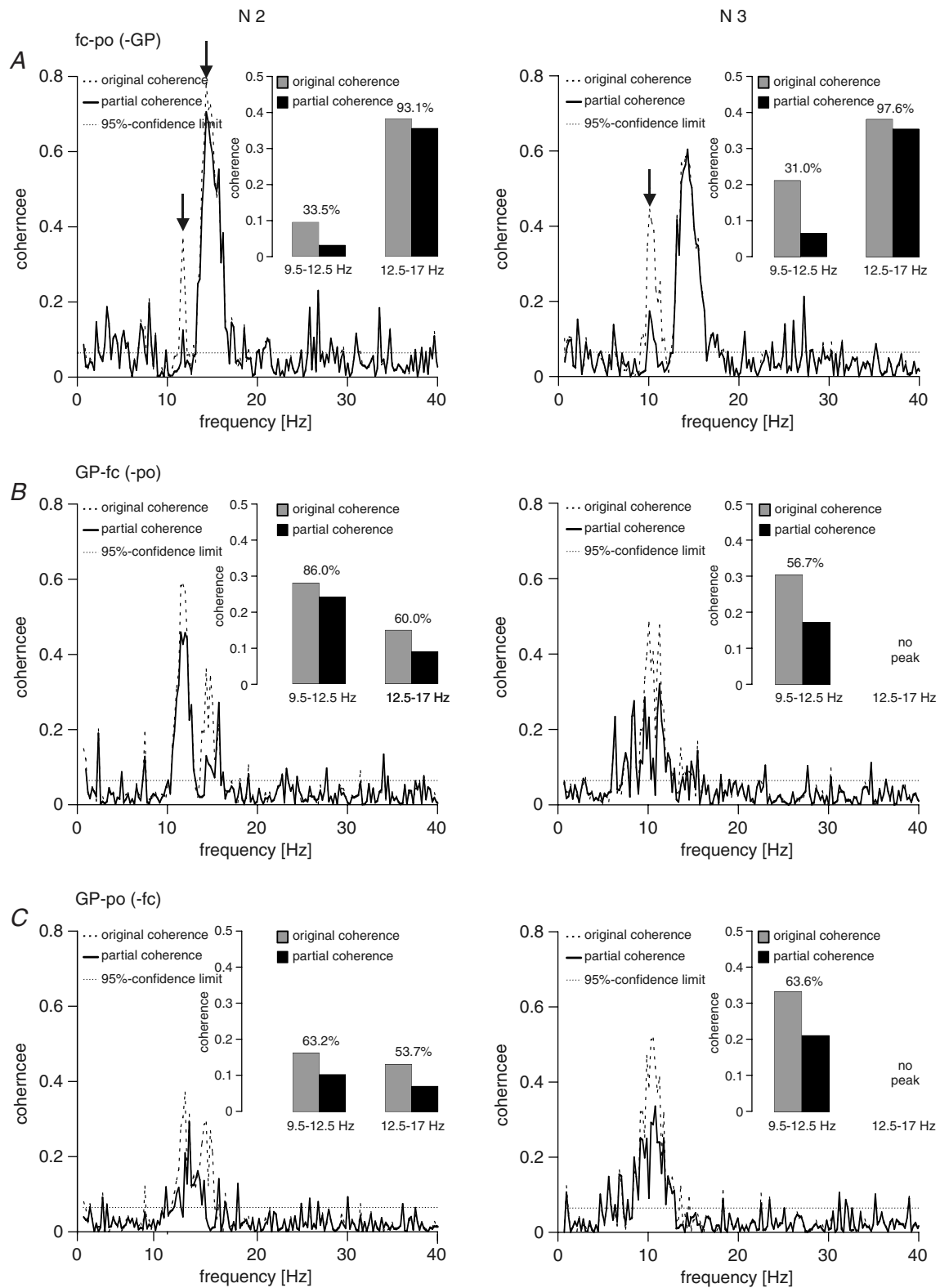


Figure 5. Example of partial coherences in one subject (same as in Fig. 1) for N2 and N3

Percentages in the bar graph insets indicate to which level of the original coherences partial coherences dropped (expressed as the percentage of the original coherence). *A*, coherence between fronto-central and parieto-occipital cortex with GP as predictor. *B*, coherence between GP and fronto-central cortex with parieto-occipital cortex as predictor. *C*, coherence between GP and parieto-occipital cortex with fronto-central cortex as predictor.

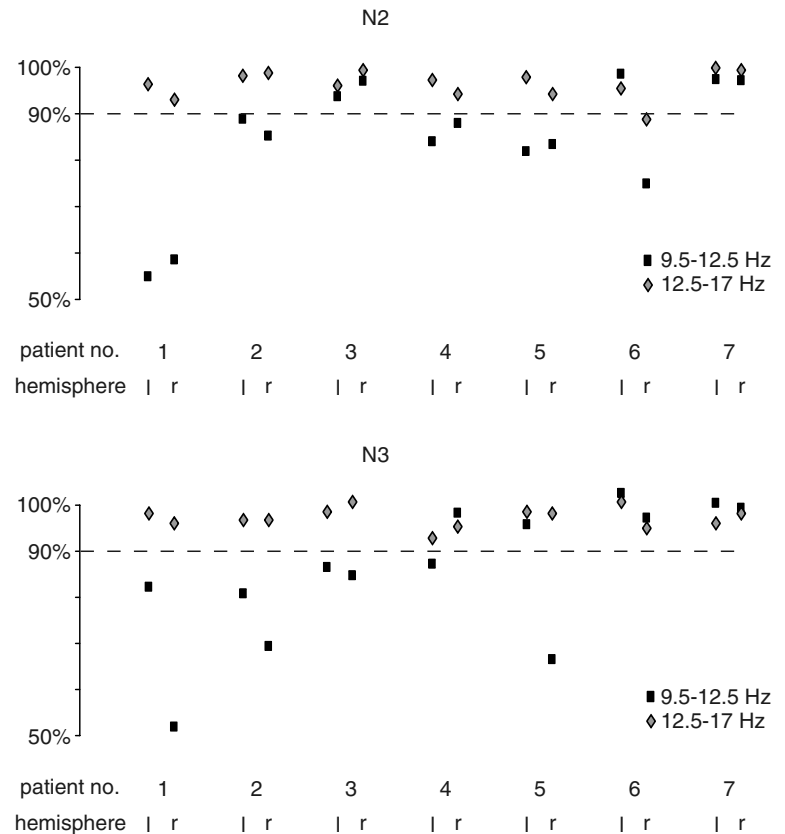


Figure 6. Drop in coherence between fronto-central and parieto-occipital cortex upon partialization with GP as predictor in each individual hemisphere for the frequency ranges of 9.5–12.5 Hz (black rectangles) and 12.5–17 Hz (grey diamonds) separately

This drop is expressed as the percentage of the remaining coherence compared to the original coherence. In N2 (A) in nine hemispheres a drop below the level of 90% in the 9.5–12.5 Hz range can be noted while in the range of 12.5–17 Hz no relevant drop occurs. In N3 (B) a drop in the 9.5–12.5 Hz range is present in eight hemispheres; again no such drop occurs in the 12.5–17 Hz range (r = right hemisphere; l = left hemisphere).

1990), it is likely that the biological phenomenon under investigation is the ~ 10 –12 Hz oscillations just outside the frequency range of ‘classical’ ~ 14 Hz sleep spindles. Like our finding of 10–12 Hz activity and the ‘alpha-delta sleep’ phenomenon, the so-called slow sleep spindles are fronto-centrally distributed (Werth *et al.* 1997). Because slow and classical spindles seem to respond differently to biological factors such as female hormones, Scheuler (1990) and Jobert *et al.* (1992) proposed different subcortical generators for the two types of oscillations.

Our study links the ~ 10 –12 Hz oscillations more specifically to the motor system in non-REM sleep. In both N2 and N3 sleep there was an appreciable drive from GP to fronto-central cortex at around ~ 10 Hz, which exceeded that from GP to parieto-occipital cortex. Moreover, controlling for the influence of GP through partialization led to a significant reduction in the coherence between fronto-central and parieto-occipital cortex at 10–12 Hz. This synchronization at 10–12 Hz seems to be specific to non-REM sleep as it has no

equivalent in the coherence spectra in wakefulness. Thus, it seems tempting to hypothesize on the functional role of 10–12 Hz activity for motor system organization during non-REM sleep. One of the key features of sleep is a state-specific inhibitory mode in the motor system which is phenomenologically reflected by muscle hypotonia during non-REM sleep and muscle atonia during REM sleep. Findings from TMS paired-pulse protocols applied in healthy sleeping subjects suggest two different modes of inhibition on the cortical level during non-REM and REM sleep (Salih *et al.* 2005). Whereas increase of cortical inhibition constitutes non-REM sleep-stages, reduction of cortical facilitation is seen during REM sleep. Based on these findings, 10–12 Hz activity as seen in our study potentially corresponds to subcortical drives that are involved in the inhibitory flow within the motor cortex during non-REM sleep. This might perhaps also explain the absence of the 10–12 Hz drive in REM sleep as inhibitory mechanisms are organized in a different way

Partialization had the biggest effect when the coherence between fronto-central and parieto-occipital cortex was considered in the 9.5–12.5 Hz range using GP as predictor (A). The effect of partialization with GP as predictor on coherence between both cortical sites was negligible in the frequency range of sleep spindles (13–17 Hz), either in N2 or N3. Using fronto-central or parieto-occipital cortex as predictor more appreciable drops were encountered in the frequency range of sleep spindles during N2 (B and C). The peaks in the 9.5–12.5 Hz and 12.5–17 Hz spindle ranges are arrowed in (A).

in that sleep stage. However, the 10–12 Hz activity may also reflect integration of coherent oscillations of motor nuclei in a basal ganglia–brainstem network that control spinal motoneurons. Studies investigating inhibitory brainstem–spinal networks in naturally sleeping cats showed increasing hyperpolarization of spinal motoneurons with the transition from non-REM to REM sleep (review: Chase & Morales, 2005). During non-REM sleep, pontine GABA-ergic neurons (e.g. nucleus pontis oralis) help to prevent glycinergic neurons in the ventromedial medulla from impinging REM-specific large inhibitory postsynaptic potentials on spinal motoneurons (Xi *et al.* 2001). Recent evidence suggests that the basal ganglia might be involved in a stage-specific manner in the supramedullary control of premotor neurons. Takakusaki *et al.* (2004) studied basal ganglia–brainstem pathways and demonstrated that projections to pontomesencephalic tegmental nuclei (especially, the pedunculopontine nucleus) are able to induce REM-like activity patterns of the pontomedullary muscle tone inhibitory system. The 10–12 Hz-activity could potentially function as an integrative motor system oscillation that contributes to activate brainstem networks that prevent REM-related inhibition of spinal motoneurons during non-REM. It constitutes a future goal to investigate whether alterations of oscillatory 10–12 Hz activity could be involved in diseases that feature pathological movements in non-REM sleep like PLMD and sleepwalking.

Conclusion

In conclusion, we propose that the motor loops of the basal ganglia–cortical circuit are functionally connected in the 10–12 Hz range in non-REM sleep, a coupling which is even enhanced with the deepening of non-REM sleep. Further, we suggest that this oscillatory phenomenon is identical to the previously described alpha–delta sleep pattern and ‘slow sleep spindles.’ Functional connectivity is also present in the δ - and sleep spindle range, but these frequency bands seem to reflect generalized oscillatory activity in non-REM sleep. With a clinical perspective in mind, it remains to be seen whether activities in different frequency bands are differently involved in the generation of sleep-related motor disorders or in parasomnias.

References

- Achermann P & Borbély AA (1998). Coherence analysis of the human sleep electroencephalogram. *Neuroscience* **85**, 1195–1208.
- American Academy for Sleep Medicine (2007). The AASM Manual for the scoring of sleep and associated events. Rules, terminology and technical specifications. American Academy of Sleep Medicine, Westchester, IL, USA.
- Astolfi L, Cincotti F, Mattia D, Babiloni C, Carducci F, Basilico A, Rossini PM, Salinari S, Ding L, Ni Y, He B & Babiloni F (2005). Assessing cortical functional connectivity by linear inverse estimation and directed transfer function: simulations and application to real data. *Clin Neurophysiol* **116**, 920–932.
- Bolam JP, Hanley JJ, Booth PA & Bevan MD (2000). Synaptic organisation of the basal ganglia. *J Anat* **196**, 527–542.
- Braun AR, Balkin TJ, Wesenten NJ, Carson RE, Varga M, Baldwin P, Belenky G & Herscovitch P (1997). Regional cerebral blood flow throughout the sleep–wake cycle. An H₂¹⁵O PET study. *Brain* **120**, 1173–1197.
- Brotini S & Gigli GL (2004). Epidemiology and clinical features of sleep disorders in extrapyramidal disease. *Sleep Med* **5**, 169–179.
- Cassidy MJ & Brown P (2003). Spectral phase estimates in the setting of multidirectional coupling. *J Neurosci Methods* **127**, 95–103.
- Chase MH & Morales FR (2005). Control of motoneurons during sleep. In *Principles and Practice of Sleep Medicine*, ed. Kryger MH, Roth T & Dement WC, pp. 154–168. Elsevier Saunders, Philadelphia.
- Chen CC, Kuhn AA, Hoffmann KT, Kupsch A, Schneider GH, Trottenberg T *et al.* (2006a). Oscillatory pallidal local field potential activity correlates with involuntary EMG in dystonia. *Neurology* **66**, 418–420.
- Chen CC, Kuhn AA, Trottenberg T, Kupsch A, Schneider GH & Brown P (2006b). Neuronal activity in globus pallidus interna can be synchronized to local field potential activity over 3–12 Hz in patients with dystonia. *Exp Neurol* **202**, 480–486.
- Contreras D, Deshexhe A, Sejnowski TJ & Steriade M (1996). Control of spatiotemporal coherence of a thalamic oscillation by corticothalamic feed back. *Science* **274**, 771–774.
- Dijk D, Roth C, Landolt H, Werth E, Aeppli M, Achermann P & Borbély AA (1995). Melatonin effect on daytime sleep in men: suppression of EEG low frequency activity and enhancement of spindle frequency activity. *Neurosci Lett* **210**, 13–16.
- Duckrow RB & Zaveri HP (2005). Coherence of the electroencephalogram during the first sleep cycle. *Clin Neurophysiol* **116**, 1088–1095.
- Finelli LA, Borbély AA & Achermann P (2001). Functional topography of the human nonREM sleep electroencephalogram. *Eur J Neurosci* **13**, 2282–2290.
- Gibbs FA & Gibbs EL (1950). *Atlas of Encephalography*, 2nd edn. Addison-Wesley Press, Cambridge.
- Grosse P, Khatami R, Salih F, Kühn A & Meyer B-U (2002). Excitability of the corticospinal system in natural human sleep as assessed by transcranial magnetic stimulation. *Neurology* **59**, 1988–1991.
- Guillery RW & Harting JK (2003). Structure and connections of the thalamic reticular nucleus: Advancing views over half a century. *J Comp Neurol* **463**, 360–371.
- Halliday DM, Rosenberg JR, Amjad AM, Breeze P, Conway BA & Farmer SF (1995). A framework for the analysis of mixed time series/point process data – theory and application to the study of physiological tremor, single motor unit discharges and electromyograms. *Prog Biophys Mol Biol* **64**, 237–278.

- Hauri P & Hawkins DR (1973). Alpha-delta sleep. *Electroencephalogr Clin Neurophysiol* **34**, 233–237.
- Jobert M, Poiseau E, Jähnig P, Schulz H & Kubicki S (1992). Topographical analysis of sleep spindle activity. *Neuropsychobiology* **26**, 210–217.
- Kaminski MJ & Blinowska KJ (1991). A new method of the description of the information flow in the brain structures. *Biol Cybern* **65**, 203–210.
- Korzeniewska A, Mańczak M, Kamiński M, Blinowska KJ & Kasicki S (2003). Determination of information flow direction among brain structures by a modified directed transfer function (dDTF) method. *J Neurosci Methods* **125**, 195–207.
- Krauss JK, Loher TJ, Weigel R, Capelle HH, Weber S & Burgunder JM (2003). Chronic stimulation of the globus pallidus internus for treatment of non-DYT1 generalized dystonia and choreoathetosis: 2-year follow up. *J Neurosurg* **98**, 785–792.
- Kupsch A, Benecke R, Müller J, Trottenberg T, Schneider GH, Poewe W, Eisner W, Wolters A, Müller JU, Deuschl G, Pinsker MO, Skogseid IM, Roeste GK, Vollmer-Haase J, Brentrup A, Krause M, Tronnier V, Schnitzler A, Voges J, Nikkah G, Vesper J, Naumann M & Volkmann J; Deep-Brain Stimulation for Dystonia Study Group (2006). Pallidal deep-brain stimulation in primary generalized or segmental dystonia. *N Engl J Med* **355**, 1978–1990.
- Kus R, Kaminski M & Blinowska KJ (2004). Determination of EEG activity propagation: pair-wise versus multichannel estimate. *IEEE Trans Biomed Eng* **51**, 1501–1510.
- Lopes da Silva FH, Vos JE, Mooibroek JN & van Rotterdam A (1980). A partial coherence analysis of thalamic and cortical alpha rhythms in dog – a contribution towards a general model of cortical organisation of rhythmic activity. In *Event Related Changes in Cortical Rhythmic Activities – Behavioural Correlates*, ed. Pfuetscheller G, pp. 33–59. Elsevier, Amsterdam.
- Lozano AM, Dostrovsky J, Chen R & Ashby P (2002). Deep brain stimulation for Parkinson's disease: disrupting the disruption. *Lancet Neurol* **1**, 225–231.
- Magill PJ, Bolam P & Bevan MD (2000). Relationship of activity in the subthalamic nucleus–globus pallidus network to cortical electroencephalogram. *J Neurosci* **20**, 820–833.
- Magill PJ, Sharott A, Bolam JP & Brown P (2004). Brain state-dependency of coherent oscillatory activity in the cerebral cortex and basal ganglia of the rat. *J Neurophysiol* **92**, 2122–2136.
- Maquet P, Degueldre C, Delfiore G, Aerts J, Péters JM, Luxen A & Franck G (1997). Functional neuroanatomy of human slow wave sleep. *J Neurosci* **17**, 2807–2812.
- Mima T, Matsuoka T & Hallett M (2001). Information flow from the sensorimotor cortex to muscle in humans. *Clin Neurophysiol* **112**, 122–126.
- Moldofsky H (1989). Sleep and fibrositis syndrome. *Rheumatic Dis Clin N Am* **15**, 91–103.
- Montagna P, Provini F & Vetrugno R (2006). Propriospinal myoclonus at sleep onset. *Neurophysiol Clin* **36**, 351–355.
- Olbrich E & Achermann P (2005). Analysis of oscillatory patterns in the human sleep EEG using a novel detection algorithm. *J Sleep Res* **14**, 337–346.
- Pivik RT & Harman KA (1995). Reconceptualization of EEG alpha activity as an index of arousal during sleep: all alpha activity is not equal. *J Sleep Res* **4**, 131–137.
- Rechtschaffen A & Kales A (1968). *A Manual of Standardized Terminology, Techniques, and Scoring System for Sleep Stages of Human Subjects*. US Department of Health, Education, and Welfare, Bethesda, MD, USA.
- Regan D (1989). *Human Brain Electrophysiology, Evoked Potentials and Evoked Magnetic Fields in Science and Medicine*. Elsevier Press, New York.
- Rosenberg JR, Halliday DM, Breeze P & Conway BA (1998). Identification of patterns of neuronal activity: partial spectra, partial coherence, and neuronal interactions. *J Neurosci Methods* **83**, 57–72.
- Salih F, Khatami R, Steinheimer S, Hummel O, Kühn A & Grosse P (2005). Inhibitory and excitatory intracortical circuits across the human sleep-wake cycle using paired-pulse TMS. *J Physiol* **565**, 695–701.
- Schaltenbrand G & Wahren W (1977). *Atlas for Stereotaxy of the Human Brain*. Thieme, Stuttgart.
- Schenck CH, Bundlie SR, Ettinger MG & Mahowald MW (1986). Chronic behavioral disorders of human REM sleep: a new category of parasomnia. *Sleep* **9**, 293–308.
- Scheuler W (1990–91). EEG sleep activities react topographically different to GABAergic sleep modulation by flunitrazepam: relationship to regional distribution of benzodiazepine receptor subtypes. *Neuropsychobiology* **23**, 213–221.
- Scheuler W, Stinshoff D & Kubicki S (1983). The alpha-sleep pattern: differentiation from other sleep patterns and effect of hypnotics. *Neuropsychobiology* **10**, 183–189.
- Sharott A, Grosse P, Kühn A, Salih F, Engel AK, Kupsch A, Schneider GH, Krauss JK & Brown P (2008). Is the synchronization between pallidal and muscle activity in primary dystonia due to peripheral afference or a motor drive? *Brain* **131**, 473–484.
- Sharott A, Magill PJ, Bolam JP & Brown P (2005). Directional analysis of coherent oscillatory field potentials in the cerebral cortex and basal ganglia of the rat. *J Physiol* **562**, 951–963.
- Steriade M (2000). Corticothalamic resonance, states of vigilance and mentation. *Neuroscience* **101**, 243–276.
- Steriade M (2001). Active neocortical processes during quiescent sleep. *Arch Ital Biol* **139**, 37–51.
- Supp GG, Schlögl A, Fiebach CJ, Gunter TC, Vigliocco G, Pfuetscheller G & Petsche H (2008). Semantic memory retrieval: cortical couplings in object recognition in the N400 window. *Eur J Neurosci* **21**, 1139–1143.
- Takakusaki K, Saitoh K, Harada H, Okumura T & Sakamoto T (2004). Evidence for a role of basal ganglia in the regulation of rapid eye movement sleep by electrical and chemical stimulation for the pedunculo-pontine tegmental nucleus and substantia nigra pars reticulata in decerebrate cats. *Neuroscience* **124**, 207–220.
- Tsoukatos J, Kiss ZH, Davis KD, Tasker RR & Dostrovsky JO (1997). Patterns of neuronal firing in the human lateral thalamus during sleep and wakefulness. *Exp Brain Res* **113**, 273–282.

- Urbain N, Gervasoni D, Soulière F, Lobo L, Rentéro, Windels F, Astier B, Savasta M, Fort P, Renaud B, Luppi P & Chouvet G (2000). Unrelated course of subthalamic nucleus and globus pallidus neuronal activities across vigilance states in the rat. *Eur J Neurosci* **12**, 3361–3374.
- Velasco M, Eugenia-Diaz-de Leon A, Máquez I, Brito F, Carrillo-Ruiz JD, Velasco AL & Velasco F (2002). Temporo-spatial correlations between scalp and centromedian thalamic EEG activities of stage II slow wave sleep in patients with generalized seizures of the cryptogenic Lennox–Gastaut syndrome. *Clin Neurophysiol* **113**, 25–32.
- Vetrugno R, Provini F & Montagna P (2006). Restless legs syndrome and periodic limb movements. *Rev Neurol Dis* **3**, 61–70.
- Villablanca J (1972). Permanent reduction in sleep after removal of cerebral cortex and striatum in cats. *Brain Res* **36**, 463–468.
- Vitek JL, Chockkan V, Zhang JY, Kaneoke Y, Evatt M, DeLong MR, Triche S, Mewes K, Hashimoto T & Bakay RA (1999). Neuronal activity in the basal ganglia in patients with generalized dystonia and hemiballismus. *Ann Neurol* **46**, 22–35.
- Volkman J & Benecke R (2002). Deep brain stimulation for dystonia: patient selection and evaluation. *Mov Disord* **17** (Suppl. 3), 112–115.
- Wennberg R & Lozano A (2003). Intracranial volume conduction of cortical spikes and sleep potentials recorded with deep brain stimulating electrodes. *Clin Neurophysiol* **114**, 1403–1418.
- Werth E, Achermann P & Borbély AA (1997). Fronto-occipital EEG power gradients in human sleep. *J Sleep Res* **6**, 102–112.
- Xi MC, Morales FR & Chase MH (2001). The motor inhibitory system operating during active sleep is tonically suppressed by GABAergic mechanisms during other states. *J Neurophysiol* **86**, 1908–1915.

Acknowledgements

F Salih was supported by a young investigators research grant from the German Society for Clinical Neurophysiology. We thank Ms Karin Reichel for her kind assistance with the EEG recordings.